Chemical Physics Letters 653 (2016) 67–72

Contents lists available at ScienceDirect

Chemical Physics Letters

journal homepage: www.elsevier.com/locate/cplett

Research paper

A femtosecond stimulated Raman spectroscopic study on the oxazine ring opening dynamics of structurally-modified indolobenzoxazines

Kipras Redeckas [a,*], Stepas Toliautas [b], Rasa Steponavičiūtė [c], Algirdas Šačkus [c], Juozas Sulskus [b], Mikas Vengris [a]

[a] Department of Quantum Electronics, Faculty of Physics, Vilnius University, Saulėtekio av. 10, LT-10223 Vilnius, Lithuania
[b] Department of Theoretical Physics, Faculty of Physics, Vilnius University, Saulėtekio av. 9, LT-10222 Vilnius, Lithuania
[c] Department of Organic Chemistry, Kaunas University of Technology, K. Baršausko St. 59, LT-50270 Kaunas, Lithuania

ARTICLE INFO

Article history:
Received 23 February 2016
Revised 25 March 2016
In final form 9 April 2016
Available online 20 April 2016

ABSTRACT

Steady-state and time-resolved femtosecond stimulated Raman scattering spectroscopic methods were applied to elucidate the photodynamics and the oxazine ring opening contingency in phenyl-substituted indolobenzoxazine systems. Using wavelength- and pulse duration-tunable multi-pulse techniques, we have measured the (static) stimulated Raman spectra of the chemically ring-opened indolobenzoxazines, and the (dynamic) femto-to-nanosecond time- and wavenumber-resolved spectra of their photo-generated species. The two experimental realizations show a notable vibronic disparity, thereby indicating the structural difference between the chemically bond-cleaved and the UV excitation produced species.

1. Introduction

Indolobenzoxazines (**IBs**) are a relatively new class of organic compounds, consisting of structurally fused indoline and benzoxazine moieties (Fig. 1(a)). **IBs** are normally assumed to be positively photochromic and their photochromism is purportedly associated with UV excitation-induced C—O bond breakage and the sub-nanosecond formation of 3H-indolium and 4-nitrophenolate chromophores, the latter of which exhibits absorption in the blue part of the visible spectrum [1–4] (even though molecular substitutions to the basic chemical structure can heavily alter the transient absorption spectra [4–6]). While numerous sub-microsecond [1–5,7] and sub-nanosecond [6,8,9] time-resolved studies have been carried out on **IB** compounds, the mechanism of their photodynamics remains unclear. Spectral discrepancies between the chemically ring-opened and the optical excitation-induced forms [1,5], prominent influence of the molecular substitutions [4–6], and the dependence of ground-state recovery times on molecular oxygen level [10,11] have recently led to suggestions that an intersystem crossing process effectively competes with the oxazine ring opening. A certain level of ambiguity stems from the fact that all time-resolved studies on **IBs** performed until now were based on electronic absorption spectra [1–13] that inherently provide very little explicit information on the structural changes of the molecule, thus suggesting that structure-sensitive spectro-temporal methods are necessary to provide additional insight on the intricate **IB** photodynamics. Moreover, the current knowledge of the vibrational behavior of the **IB** species is rather scarce. In this letter we aim to address these issues by presenting an experimental study, elucidating the vibrational statics and dynamics of **IBs**. We employ femtosecond stimulated Raman scattering (FSRS) spectroscopic techniques [14–17] to analyze the ground- and the photoexcited-state vibrational development of several selected **IBs**. These experiments shed additional insight to the **IB** photophysics and, to our knowledge, this is the first vibrational study on compounds of the **IB** family.

2. Materials and methods

For the study, we have selected several previously investigated [5,6,8,10] **IB** compounds with phenylic substituents in the *para*-position, relative to the nitrogen of the indole ring: **IB1** (4-methoxyphenyl substitution, orange structure in Fig. 1(a)) and **IB2** (3-chlorphenyl[1] substitution, blue structure in Fig. 1(a)). These compounds were chosen mainly for their relatively high quantum yield [5], compared to numerous other **IBs** [1–3,7,13], and excellent

* Corresponding author.
E-mail address: kipras.redeckas@ff.vu.lt (K. Redeckas).

[1] For interpretation of color in figures, the reader is referred to the web version of this article.

http://dx.doi.org/10.1016/j.cplett.2016.04.030
0009-2614/

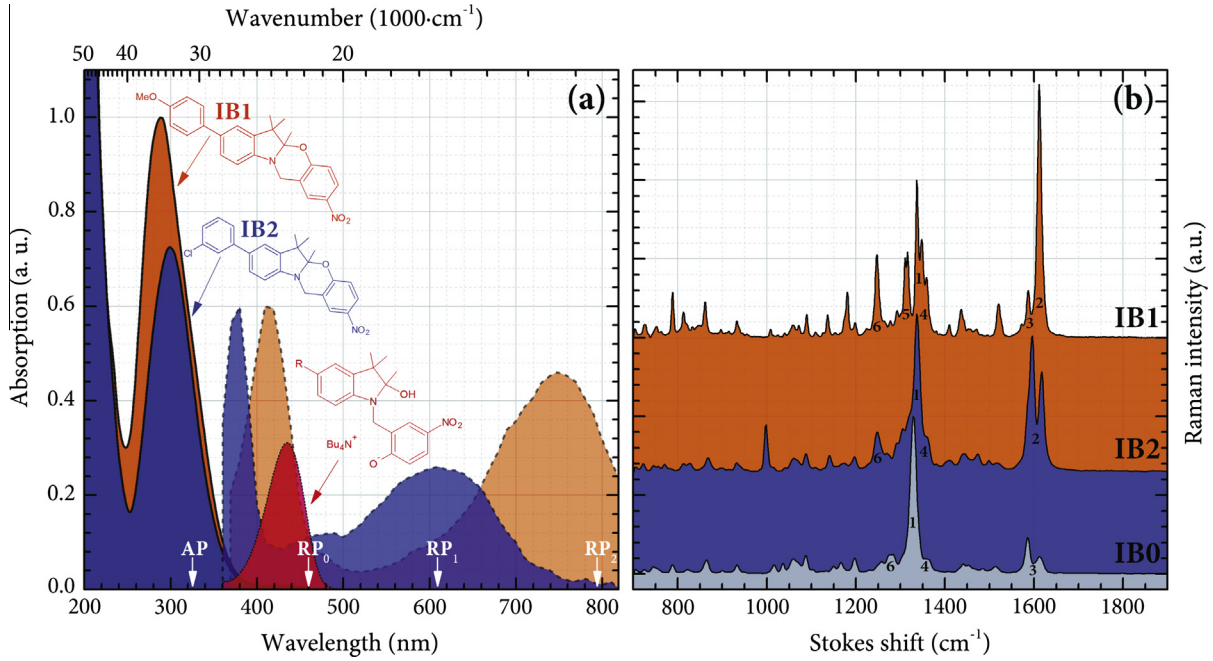

Fig. 1. (a) Steady-state (solid lines, opaque plot area) and excited-state [5,6] (dashed lines, transparent plot area) absorption spectra of the phenyl-substituted indolobenzoxazine compounds **IB1** (orange[1]) and **IB2** (blue) dissolved in acetonitrile (the dotted line/semi-transparent red plot represents the NUV/VIS part of the chemically-opened form steady-state absorption spectrum [5]). The molecular structures of the compounds are presented adjacent to the proper spectra; arrows on the bottom abscissa indicate spectral positions of the actinic and the Raman pump pulses. (b) Steady state spontaneous Raman scattering spectra of compounds **IB1**, **IB2**, and the unsubstituted indolobenzoxazine **IB0** [1,2,9]. The spectra are offset vertically and normalized with respect to the ca. 1330 cm^{-1} —NO_2 band for better viewing. Numbers indicate the positions of several significant spectral peaks (Table 1).

photodynamical stability [5]. The unsubstituted ("base") indolobenzoxazine compound **IB0** [1–3,9] was, for comparative purposes, studied only via steady-state (i.e., SRS) techniques, since its lower quantum yield [1–3] and fatigue resistance [5] proved to be inadequate for time-resolved FSRS measurements (which necessitated higher excitation intensities to produce a feasible amount of the excited state population). The ground state absorption of the phenyl-substituted **IBs** peaks at ca. 290–300 nm, while the transient absorption of their photo-induced forms is distinctive for its double-band structure, peaking in the UV/VIS (415 nm for **IB1** and 375 nm for **IB2**) and the VIS/NIR (750 nm for **IB1** and 600 nm for **IB2**) boundaries. These spectra are in striking contrast to the ones of the chemically-induced ring-opened forms (produced via addition of tetrabutylammonium hydroxide (TBAH) to the sample solutions [1–3,5,10]) that exhibit only a single spectral maximum in the VIS/NIR, peaking for both compounds at ca. 430 nm [5,6,10] (red spectrum in Fig. 1(a)).

FSRS experiments were performed using a home-built spectroscopic setup introduced in [18]. In short, FSRS is a multi-pulse technique in which a narrowband (picosecond) pulse, resonant to an electronic transition of the sample, induces resonant Raman scattering, while a time-coincident broadband (femtosecond) pulse triggers stimulated Raman emission, thereby giving rise to Stokes (and anti-Stokes) features on top of the probe field [15,16,19]. If an auxiliary, temporally-variable femtosecond pulse is used to excite the sample (and the Raman pump is set to correspond to an excited state resonance), FSRS can be utilized to measure the time-dependent vibrational dynamics of the evolving system with both excellent temporal and spectral resolution [15–17,19]. Two different types of SRS measurements were performed on the **IB** compounds: (a) steady state SRS (without the actinic pulse) on the chemically ring-opened **IB** forms (i.e., investigation of the characteristic Raman frequencies of the blue-absorbing ring-opened molecule); and (b) time-resolved FSRS on the photoexcited **IB** species (i.e., investigation of the time-dependent vibrational changes, occurring after the UV photon absorption). Crystalline **IB** samples were dissolved in acetonitrile (*Lichrosolv Gradient Grade*) and diluted to an appropriate concentration for the either of the experiments. In the time-resolved FSRS experiments both of the **IB** samples, concentrated to 1 OD at 325 nm in a 1 mm optical pathway, were excited with λ_{AP} = 325 nm, E_{AP} = 1 μJ, τ_{AP} = 70 fs actinic pulses, while the Raman pumps were set to either λ_{RP} = 795 nm, E_{RP} = 5 μJ, τ_{RP} = 3.5 ps for **IB1**, or λ_{RP} = 610 nm, E_{RP} = 4 μJ, τ_{RP} = 4 ps for **IB2**. In the steady-state SRS experiments the concentrations were slightly increased in order to produce a sufficient amount of ring-opened species via introduction of a small amount (ca. 10 μL) of highly-concentrated TBAH (1.0 M in methanol, *Alfa Aeser*) to the **IB** solutions. Samples of 1 OD at 450 nm were used in the steady-state SRS measurements. The ground-to-excited state SRS resonance was achieved with λ_{RP} = 460 nm, E_{RP} = 2 μJ, τ_{RP} = 2 ps spectrally-narrowed pulses.

A computational study was conjointly performed to characterize the fundamental vibrational modes of the investigated **IBs**. Molecular structures of the **IB** compounds in ground electronic state were optimized using density-functional theory [20] with B3LYP functional [21] and cc-pVTZ basis set [22]. Vibrational frequency analysis including anharmonic corrections [23] and calculation of Raman scattering activities were carried out for the optimized structures. Calculations were performed using Gaussian09 package [24], using computational resources at the High Performance Computing Center "HPC Sauletekis" (Vilnius University, Faculty of Physics). Obtained scattering activities were subsequently converted to simulated Raman intensities by calculating scattering cross-section [25] (λ_0 and T values were taken from corresponding experiments).

Table 1
Calculated properties of steady-state Raman scattering of **IB** compounds. The relative intensities can be assessed from Fig. 1(b). A full list of characteristic vibrational frequencies is presented in SM.

No.	Intensity	**IB0**	**IB1**	**IB2**	Description
1.	Very strong	1334	1331	1332	NO_2 deformation
2.	Very strong	–	1604	1588, 1609	Biphenyl ring stretching along axis
3.	Strong	1585, *1615*	*1582*	*1583*	Phenyl ring and NO_2 stretching
4.	Strong	1315–1360	1315–1360	1315–1360	CH_2 out-of-plane deformations
5.	Strong	–	1282, 1306	1282	Biphenyl ring CH rocking/twisting
6.	Strong	*1233*	1237	1237	Various CH bends

The values in italics denote peaks of a given character that are less pronounced in the corresponding compounds.

3. Results and discussion

The ground state spontaneous Raman scattering spectra[2] of the phenyl-substituted **IBs** (Fig. 1(b)) feature a multitude of vibrational bands, most prominent of which surface at ca. 1330 cm^{-1} and 1600 cm^{-1}. The intense vibrations at 1330 cm^{-1} are observed in all compounds of the **IB** variety and can be ascribed to the symmetric —NO_2 stretching in the nitrophenole moiety [26,27]. While the 1600 cm^{-1} region also envelops the relatively weaker antisymmetric —NO_2 vibrations [26] (as exhibited by the unsubstituted **IB0**), the substantially intensified vibrations of **IB1** and **IB2** that arise in the particular spectral vicinity are of a different origin. The intense ~1600 cm^{-1} vibrations in the substituted **IBs** stem from the phenylic extensions of the molecule and can be ascribed to the biphenyl-like symmetric inter-aromatic ring stretching in the phenyl-indole moiety [28–31]. The phenylic substituents also give rise to reasonably intense aromatic ring rocking/twisting vibrations appearing in the close proximity of the —NO_2 peak at ca. 1280–1300 cm^{-1}. Ascription of the key vibrational modes is outlined in Table 1, whereas a full list can be found in supplementary material (SM).

In Fig. 2 we can see that in spite of the alterations to the molecular backbone (and the eventual differences emanating in the electronic excited state evolution [5,6,8,9]), the chemically-induced open-ring conformations of all the investigated compounds exhibit virtually identical SRS spectra. This equivalence allows us to assume that the SRS features in Fig. 2 belong mainly to the 4-nitrophenolate moiety, considering that the blue-absorbing ionic chromophore is predominantly resonant with the 460 nm Raman pump (for explicitness, properly scaled SRS lines of the solvent are presented in Fig. 2; the indole segment of the cleaved molecule is an unlikely candidate to be stimulated by the utilized Raman pump, as it absorbs principally in the UV [9,32,33]). The majority of the higher frequency (>1000 cm^{-1}) vibrational bands, that accompany the chemical ring opening, generally correlate with the ones observed upon the deprotonation of 4-nitrophenole [34,35]. While there are some discrepancies between the absolute positions and the relative amplitudes, in view of the main 4-nitrophenolate spectral peaks [34,35], the general outline of the Raman spectrum is, by and large, similar. Most notably, formation of 4-nitrophenolate prompts a decline of the intense ~1330 cm^{-1} —NO_2 vibrations that redshift [34] and, likely, change their vibrational character [35] following the reaction. Moreover, the SRS signals at ca. 1400–1600 cm^{-1} are common to all of the **IB** compounds, including the unsubstituted **IB0**. This suggests that in the ring-opened forms they stem from the 4-nitrophenolate-like C—O^-, C—C and C—H [34] vibrations (since the intense phenyl-indole vibrations, that occupy the same spectral region in Fig. 1(b), cannot surface in the SRS spectrum of the unsubstituted **IB0**). The chemically-opened forms are also characteristic for their two intense Raman bands, emerging at 790 and 930 cm^{-1}. Interestingly, none of the particular bands can be associated exclusively with formation of the 4-nitrophenolate moiety. While 4-nitrophenolate does in fact exhibit a singular intense lower-frequency Raman peak [34,35] (i.e., joint —NO_2 and C—C vibrations at 858 cm^{-1} [34]) the SRS peaks in Fig. 2 are interspersed from the "expected" spectral location by ±70 cm^{-1} (which is somewhat too large to be interpreted as Fermi resonance splitting of the band). While it is unclear whether these two bands appear due to either the probable upshift of the said mode, accompanied by an intensification of the ring-breathing in the indole fragment at ca. 760 cm^{-1} [36], or the possible intra-chromophore vibrations, developing intrinsically from the C—O bond dissociation, it is nonetheless evident that the emergence of these intensive Raman modes is one of the key "identifiers" of the ring-opening of an **IB** molecule.

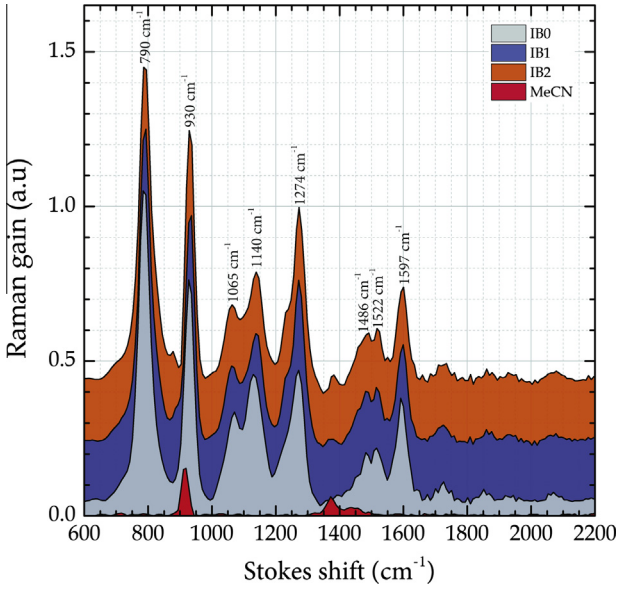

Fig. 2. Baseline- and solvent line-corrected ground state SRS spectra of the chemically ring-opened forms (via addition of TBAH to the sample solutions) of **IB1**, **IB2** and the unsubstituted indolobenzoxazine compound **IB0**. The resulting anionic nitrophenolate-like forms exhibit strong absorption at ca. 430 nm (red[1] spectrum in Fig. 1(a)) that allows us to exploit the 460 nm resonant enhancement conditions (RP_0 in Fig. 1a). The SRS spectra are normalized and offset vertically for better viewing. Red spectrum depicts the properly scaled (according to the 2250 cm^{-1} C≡N line) spectrum of acetonitrile.

In contrast to the multitude of well-defined spectral peaks of the chemically-induced open-ring forms, the time- and wavenumber-resolved FSRS datamaps in Fig. 3 indicate the presence of a single dominant vibrational band that prevails through both the early and the late stages of the **IB** photoevolution. It should be noted that

[2] Tunability of narrowband Raman pump in our FSRS setup is limited to ~400 nm on the short-wave side, which disallows resonant enhancement of the UV-absorbing **IB** solutions (Fig. 1(a)). Spontaneous Raman scattering spectra of crystalline **IB** samples were measured as an alternative. Refer to the supplementary material for the experimental details on the spontaneous Raman scattering measurements.

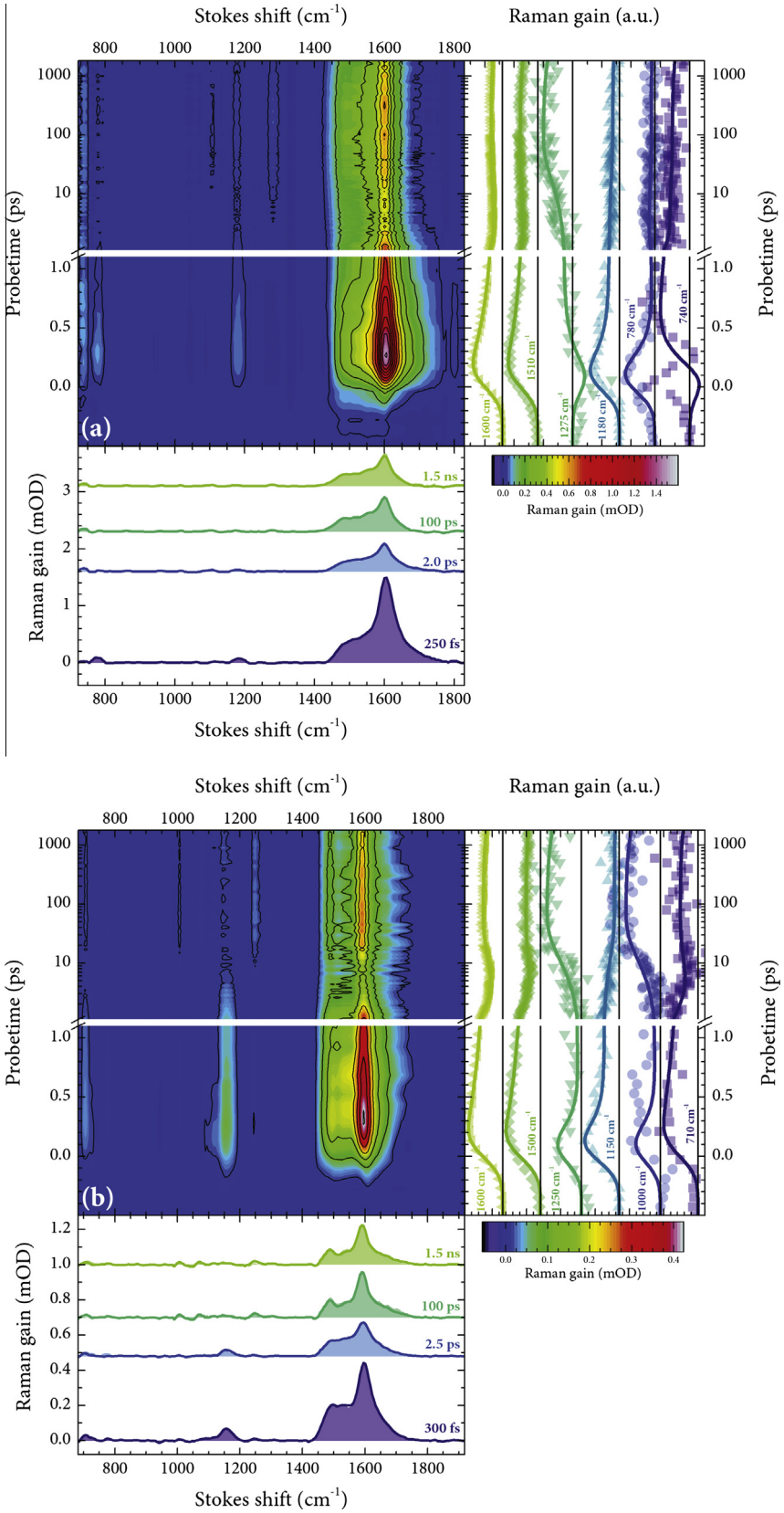

Fig. 3. FSRS spectra of compounds (a) **IB1** (λ_{RP} = 610 nm), and (b) **IB2** (λ_{RP} = 795 nm). The entire experimentally-resolved and background-corrected FSRS signals are presented in the central graphs, whereas the right-hand side and bottom graphs depict, accordingly, spectral and temporal cuts of the FSRS dataset. Note that the time-gated FSRS spectra (bottom) are offset vertically from the zero line, and the kinetic curves (right-hand side) are offset vertically and normalized for better viewing. Experimentally-resolved points are presented in discrete symbols and area-filled curves, while the continuous lines in all of the graphs represent results of a four component global fit of the experimental data (see Table SM-C1 for more details)[1].

due to the relatively low Raman yield of the **IB** samples, as well as the significant deviation of both 610 and 795 nm Raman pumps from the ground state resonances (>15,000 cm^{-1}), bleaching contributions do not surface in either of the time-gated FSRS spectra. This observation, along with the fact that the pre-actinic pump interaction FSRS signals are zero, allows us to designate all the Raman gain signals in Fig. 3 entirely to the excited and/or photoproduct states [6,8] of the investigated **IBs**. The distinguishing broad Raman peak emerges at 1606 cm^{-1} for **IB1** and at 1595 cm^{-1} for **IB2**, and is adjoined by a cluster of near-lying lower-frequency vibrational bands at ca. 1400–1500 cm^{-1}. At least two clear-cut Raman maxima on the red wing of the main peak—at 1490 and 1540 cm^{-1}—can be discerned for **IB2**, whereas the corresponding maxima of **IB1** are slightly more dispersed spectrally, indicating a potential contribution of hot luminescence [14,37], instigated by the repopulation of higher excited states of the compound [8]. Femtosecond time-resolved studies have previously shown that **IB**-type compounds exhibit a sub-picosecond decay and consequent sub-nanosecond growth of the transient absorption signal [6,9]. As observed in Fig. 3, the temporal behavior of the **IB1** and **IB2** FSRS bands in the spectral vicinity of ~1600 cm^{-1} (and, to an extent, at the lower-frequency shoulder at ~1500 cm^{-1}) clearly mimics the familiar rise-fall–rise-fall dynamics of the transient electronic absorption signals [6,8,9] and is well described by the same kinetic model (Table SM-C1). Moreover, spectral evolution during the sub-50-picosecond period distinctly shows the peak-shift to lower frequencies (by ~7 cm^{-1}) and band-narrowing phases. These FSRS dynamics, similarly to those observed in other molecules (e.g., in various carotenoids [38–40]), can be attributed to the vibrational relaxation, which, in our case, accompanies the formation of the photoproduct (also suggested in Ref. [6]). The ratios between the initial (~300 fs) and the final (~100 ps) spectral amplitudes at 1600 cm^{-1} slightly differ from the ones of the "pure" electronic signals [6,8] (also a discrepancy between the intermediate state lifetimes (see Table SM-C1) and the ones from [6] can be acknowledged), which can be explained by the fact that the Raman pumps can likewise irreversibly relocate the excited state/photoproduct population, thereby, partially altering the "standard" photoevolution [8] (also observed in other multi-pulse experiments [41,42]). Some of the more notable vibrational modes, accompanying the excited-state-to-photoproduct transition, are observed in the spectral region of ca. 750–1200 cm^{-1}. The vibrational frequencies at ca. 780 and 1180 cm^{-1} (**IB1**) and ca. 1000 and 1250 cm^{-1} (**IB2**) can be associated with the initial Frank–Condon and the singlet excited states, as suggested in [6], seeming as they rapidly decay within the first picosecond of the photoevolution. Likewise, the most prominent vibrational modes of the final forms can be identified at ca. 1275 cm^{-1} (**IB1**), and 1000 and 1250 cm^{-1} (**IB2**), acknowledging their growth in amplitude (and the escalation above their initial amplitudes) for the first 100 ps, which coincides with the formation of the final evolutionary forms [6]. On the whole, the majority of these Raman signals, as indicated by bottom graphs of Fig. 3, are almost an order of magnitude less intense than the main 1600 cm^{-1} maxima. It should also be mentioned that no clear-cut spectro-temporal activity is observed in the spectral vicinity of the main —NO_2 band at ~1330 cm^{-1}. The post-excitation behavior (i.e., bleach recovery and peak-shift) of the nitro functional group was shown to accompany the ring-opening dynamics of the related photochromic nitro-spiropyrans [43,44], and, bearing in mind the steady state vibrational changes of 4-nitrophenol [34,35], a similar effect can also be expected upon the ring-opening of **IBs**. Nonetheless, the data in this particular spectral region is less "reliable", as it lies in the close proximity of the comparatively strong 1375 cm^{-1} C—H deformation frequency of acetonitrile and is more susceptible to the solvent line subtraction artifacts [17,19].

Comparing all the presented data, one can notice an inherent dissimilarity between the chemically and optically generated **IB** forms. While the contrast between the steady-state and transient electronic absorption of the chemically- and photo-generated species has been addressed previously (Refs. [5,6,10] and Fig. 1(a)), the SRS data in Fig. 3 indicate that the particular molecular forms also bear very little vibrational semblance. This implies that although the general vibronic features of the chemically-induced forms can be ascribed to 4-nitrophenolate [34,35], the same assumption cannot be explicitly made about the forms produced via a UV photon absorption. Essentially, none of the characteristic low-to-mid-frequency (<1400 cm^{-1}) components correlate between the SRS/FSRS spectra of the two (expectedly equivalent) molecular forms. Principally, all time-resolved FSRS spectra in Fig. 3 peak in the close proximity of the characteristic higher-frequency ground state maxima (Fig. 1(b)). Moreover, this tendency is exhibited not only by compounds **IB1** and **IB2**, but also by many other *para*-substituted **IBs**, including the ones investigated in Ref. [5] (see Fig. SM-B1). Acknowledging the key contribution of phenyl-indole inter-ring vibrations to the ground state Raman spectra (Fig. 1(b)), it is safe to assume that the signals at ca. 1600 cm^{-1}, emerging in the post-excitation FSRS dynamics, also originate from vibrations of the same molecular moiety. Since these biphenyl-like vibrations are not bleached after the optical excitation (as the FSRS signal in Fig. 3 is always positive), the temporal development of the 1600 cm^{-1} region can be interpreted as an intensification of molecular vibrations (that stems from the possible electronic excitation re-localization) within the phenyl-indolic moiety. The signals that could be potentially linked to oxazine ring opening (i.e., the sub-100-picosecond growth at ~1250 cm^{-1} in Fig. 3) are much weaker than the ones assumedly associated with the phenyl-bearing fragments. These observations agree well with the earlier predictions that the UV excitation does not, in fact, cause a C—O bond breakage or (spectrally-resolvable) 4-nitrophenolate formation in photoexcited **IB** systems (especially in an acetonitrile environment [10]). It has been suggested that intersystem crossing competes with ring opening in both the substituted and unsubstituted **IBs** [10]. While the presented FSRS data supports the notion that ring-opening is not a likely outcome from UV excitation, the overwhelming biphenyl-like nature of the ground- and excited-state FSRS dynamics of the phenyl-substituted **IBs** allows us to propose yet another possible photoevolutionary route. The transient electronic absorption spectra in Fig. 1(a) bear a striking semblance to the radical forms of biphenyl and its various derivatives [29–31,45,46] (obtained both via optical excitation [29,30] and pulse radiolysis [31,45] experiments). Most specifically, both electronic species display a presence of two characteristic spectral bands – a sharp NUV/VIS peak and a broad NIR maximum. Moreover, the transient Raman spectra [30,47,48] of the said radicals also share a great deal of likeness to the ones depicted in Fig. 3 (i.e., an increased Raman activity at ν > 1500 cm^{-1}). Acknowledging the earlier observations, concerning the dependence of the sub-nanosecond dynamics on the UV excitation wavelength [6] and the susceptibility of the sub-microsecond relaxation rate to molecular oxygen [10,11], it is possible to predict that the photoexcited phenyl-substituted **IB** systems develop a biphenyl radical-like (ionic) state (or, possibly, a charge-separated form, in which the electron traverses from one of the chromophoric segment to the other) that predominates throughout the entire photoevolution. The radical formation, most likely, develops not from the excited singlet state, familiar to most **IBs** [6,8]. The unsubstituted **IB0** has also been found to decay faster in the presence of oxygen [10], which suggests that the photopathway of the substituted systems is, presumably, singlet → triplet → radical. The proposed radical nature, all things considered, would elucidate why the basic photophysical properties of the phenyl-substituted **IBs**—the noticeably higher yield [5,6], the exci-

tation saturation dynamics [5], the atypical multi-peak transient absorption spectra [5,6], and the strong contrast to 4-nitrophenolate [34,35]—are drastically different from numerous close counterparts of the **IB** family [1–7,9–13].

4. Conclusions

We have performed an experimental FSRS study on the chemically-induced and the optically-generated molecular forms of phenyl-substituted **IBs**. The vibrational (as well as the electronic [5,6,8,10]) spectra of the "factual" ring-opened molecules show an inherent similarity to 4-nitrophenolate [1–3,34,35], whereas the UV excitation generated species exhibit a singular dominant vibrational peak at ca. 1600 cm^{-1}. The latter results suggest an increased vibrational activity within the phenyl-indolic (and not the nitrophenolic) moiety, thus indicating that the substituents heavily alter the vibronic photodynamics of **IB** systems. The FSRS data support the earlier assumptions [10,11] that the ring-opening competes with an auxiliary electronic process. Moreover, the peculiar FSRS activity within the indolic fragment of the molecule allows us to estimate that the UV-generated excited state species might actually be not of a triplet (as suggested in [10,11]), but of a ionic radical-like [30,46,47] character.

Acknowledgements

The authors would like to thank prof. Valdas Šablinskas from Department of General Physics and Spectroscopy (Vilnius University) and prof. Gediminas Niaura from Department of Organic Chemistry (Center for Physical Sciences and Technology) for the steady state spontaneous Raman scattering measurements.

Appendix A. Supplementary material

Supplementary data associated with this article can be found, in the online version, at http://dx.doi.org/10.1016/j.cplett.2016.04.030.

References

[1] M. Tomasulo, S. Sortino, F.M. Raymo, J. Photochem. Photobiol. A 200 (2008) 44.
[2] M. Tomasulo, S. Sortino, F.M. Raymo, J. Org. Chem. 73 (2008) 118.
[3] M. Tomasulo, S. Sortino, A.J.P. White, F.M. Raymo, J. Org. Chem. 70 (2005) 8180.
[4] E. Deniz, M. Tomasulo, S. Sortino, F.M. Raymo, J. Phys. Chem. C 113 (2009) 8491.
[5] V. Voiciuk, K. Redeckas, V. Martynaitis, R. Steponavičiūtė, A. Šačkus, M. Vengris, J. Photochem. Photobiol. A 278 (2014) 60.
[6] K. Redeckas, V. Voiciuk, R. Steponavičiūtė, V. Martynaitis, A. Šačkus, M. Vengris, J. Photochem. Photobiol. A 285 (2014) 7.
[7] M. Tomasulo, E. Deniz, T. Benelli, S. Sortino, F.M. Raymo, Adv. Funct. Mater. 19 (2009) 3956.
[8] K. Redeckas, V. Voiciuk, R. Steponavičiūtė, V. Martynaitis, A. Šačkus, M. Vengris, J. Phys. Chem. A 118 (2014) 5642.
[9] M. Barkauskas, V. Martynaitis, A. Šačkus, R. Rotomskis, V. Sirutkaitis, M. Vengris, Lith. J. Phys. 48 (2008) 231.
[10] V. Voiciuk, K. Redeckas, V. Martynaitis, R. Steponaviciute, A. Sackus, M. Vengris, PCCP 17 (2015) 17828.
[11] F.M. Raymo, J. Phys. Chem. A 116 (2012) 11888.
[12] M. Tomasulo, S. Sortino, F.M. Raymo, Adv. Mater. 20 (2008) 832.
[13] M. Tomasulo, S. Sortino, A.J.P. White, F.M. Raymo, J. Org. Chem. 71 (2006) 744.
[14] S.-Y. Lee, D. Zhang, D.W. McCamant, P. Kukura, R.A. Mathies, J. Chem. Phys. 121 (2004) 3632.
[15] P. Kukura, D.W. McCamant, R.A. Mathies, Annu. Rev. Phys. Chem. 58 (2007) 461.
[16] D.W. McCamant, P. Kukura, R.A. Mathies, Appl. Spectrosc. 57 (2003) 1317.
[17] D.W. McCamant, P. Kukura, S. Yoon, R.A. Mathies, Rev. Sci. Instrum. 75 (2004) 4971.
[18] K. Redeckas, V. Voiciuk, M. Vengris, Photosynth. Res. 128 (2016) 169.
[19] D.W. McCamant, P. Kukura, R.A. Mathies, J. Phys. Chem. A 107 (2003) 8208.
[20] R.G. Parr, Density-Functional Theory of Atoms and Molecules, Oxford University Press, USA, 1989.
[21] P.J. Stephens, F.J. Devlin, C.F. Chabalowski, M.J. Frisch, J. Phys. Chem. 98 (1994) 11623.
[22] R.A. Kendall, T.H. Dunning, R.J. Harrison, J. Chem. Phys. 96 (1992) 6796.
[23] V. Barone, J. Chem. Phys. 122 (2005) 014108.
[24] M.J. Frisch, G.W. Trucks, H.B. Schlegel, G.E. Scuseria, M.A. Robb, J.R. Cheeseman, G. Scalmani, V. Barone, B. Mennucci, G.A. Petersson, H. Nakatsuji, M. Caricato, X. Li, H.P. Hratchian, A.F. Izmaylov, J. Bloino, G. Zheng, J.L. Sonnenberg, M. Hada, M. Ehara, K. Toyota, R. Fukuda, J. Hasegawa, M. Ishida, T. Nakajima, Y. Honda, O. Kitao, H. Nakai, T. Vreven, J.A. Montgomery Jr., J.E. Peralta, F. Ogliaro, M.J. Bearpark, J. Heyd, E.N. Brothers, K.N. Kudin, V.N. Staroverov, R. Kobayashi, J. Normand, K. Raghavachari, A.P. Rendell, J.C. Burant, S.S. Iyengar, J. Tomasi, M. Cossi, N. Rega, N.J. Millam, M. Klene, J.E. Knox, J.B. Cross, V. Bakken, C. Adamo, J. Jaramillo, R. Gomperts, R.E. Stratmann, O. Yazyev, A.J. Austin, R. Cammi, C. Pomelli, J.W. Ochterski, R.L. Martin, K. Morokuma, V.G. Zakrzewski, G.A. Voth, P. Salvador, J.J. Dannenberg, S. Dapprich, A.D. Daniels, Ö. Farkas, J.B. Foresman, J.V. Ortiz, J. Cioslowski, D.J. Fox, Gaussian 09, Revision D.01. Gaussian Inc, Wallingford, CT, USA, 2013.
[25] D. Michalska, R. Wysokiński, Chem. Phys. Lett. 403 (2005) 211.
[26] D. Lin-Vien, N.B. Colthup, W.G. Fateley, J.G. Grasselli, The Handbook of Infrared and Raman Characteristic Frequencies of Organic Molecules, Academic Press, San Diego, USA, 1991.
[27] A. Kovács, V. Izvekov, G. Keresztury, G. Pongor, Chem. Phys. 238 (1998) 231.
[28] P. Sett, S. Chattopadhyay, P.K. Mallick, Chem. Phys. Lett. 331 (2000) 215.
[29] C. Kato, H.-O. Hamaguchi, M. Tasumi, Chem. Phys. Lett. 120 (1985) 183.
[30] G. Buntinx, O. Poizat, J. Chem. Phys. 91 (1989) 2153.
[31] J. Choi, D.W. Cho, S. Tojo, M. Fujitsuka, T. Majima, J. Phys. Chem. A 119 (2015) 851.
[32] M.W. Allen, J.R. Unruh, B.D. Slaughter, S.J. Pyszczynski, T.R. Hellwig, T.J. Kamerzell, C.K. Johnson, J. Phys. Chem. A 107 (2003) 5660.
[33] L. Serrano-Andrés, B.O. Roos, JACS 118 (1996) 185.
[34] R.A. Ando, A.C. Borin, P.S. Santos, J. Phys. Chem. A 111 (2007) 7194.
[35] M. Muniz-Miranda, Appl. Catal. B 146 (2014) 147.
[36] S.D. Dieng, J.P.M. Schelvis, J. Phys. Chem. A 114 (2010) 10897.
[37] B. Zhao, K. Niu, X. Li, S.-Y. Lee, Sci. China Chem. 54 (2011) 1989.
[38] S. Shim, R.A. Mathies, J. Phys. Chem. B 112 (2008) 4826.
[39] T.M. Kardaś, B. Ratajska-Gadomska, A. Lapini, E. Ragnoni, R. Righini, M. Di Donato, P. Foggi, W. Gadomski, J. Chem. Phys. 140 (2014) 204312.
[40] M. Kloz, R.v. Grondelle, J.T.M. Kennis, PCCP 13 (2011) 18123.
[41] A. Weigel, A. Dobryakov, B. Klaumünzer, M. Sajadi, P. Saalfrank, N.P. Ernsting, J. Phys. Chem. B 115 (2011) 3656.
[42] S. Ruetzel, M. Kullmann, J. Buback, P. Nuernberger, T. Brixner, Phys. Rev. Lett. 110 (2013) 148305.
[43] J. Buback, M. Kullmann, F. Langhojer, P. Nuernberger, R. Schmidt, F. Würthner, T. Brixner, JACS 132 (2010) 16510.
[44] A.-K. Holm, M. Rini, E.T.J. Nibbering, H. Fidder, Chem. Phys. Lett. 376 (2003) 214.
[45] K. Sehested, E.J. Hart, J. Phys. Chem. 79 (1975) 1639.
[46] C. Takahashi, S. Maeda, Chem. Phys. Lett. 24 (1974) 584.
[47] T. Nakabayashi, S. Kamo, H. Sakuragi, N. Nishi, J. Phys. Chem. A 105 (2001) 8605.
[48] Y. Sasaki, H.-O. Hamaguchi, Spectrochim. Acta Mol. Biomol. Spectrosc. 50 (1994) 1475.